Table of Contents

Title: Development of a Mars ionosphere model with time-dependent solar forcing for studies of solar flare effects

Short title: Solar flares on Mars

Summary of proposal:

We propose to develop a Mars ionosphere model with time-dependent solar forcing and to use it to compare predictions and observations of the ionospheric effects of solar flares. Solar flares are "active experiments" that probe the response of the martian ionosphere to extreme conditions. The proposed improvements will strengthen one of the weakest areas in current models, the bottomside ionosphere. The Mars ionosphere represents the interface between the neutral atmosphere, driven by seasonal obliquity and dust cycles, and the space plasma environment, driven by the solar wind and crustal magnetic fields. Many escaping particles come from the ionosphere, making ionospheric processes important for the history of volatiles on Mars. Solar flares can impact mission operations because they cause increased radio wave absorption, which impacts communications

Our basic research plan is:
Adapt existing 1-D Mars ionosphere model to permit time-variable solar irradiances and various models of photoelectron-impact ionization.
Acquire solar spectra with good spectral and temporal range and resolution.
Run simulations to produce vertical profiles of ion and electron densities as functions of time.
Adjust models of photoelectron-impact ionization to optimize fit between observations and simulations.
Draw conclusions about the effects of solar flares on the Mars ionosphere.
Draw conclusions about how photoelectron-impact ionization controls the bottomside Mars ionosphere.
Draw conclusions about the physical process of photoelectron-impact ionization that are transferable to all ionospheres.

Summary of personnel and effort:

Name	Role	Institution	Funded Effort per year	Unfunded Effort per year
Dr. Paul Withers	PI	Boston Univ.	4 months	0
Majd Matta	Grad student	Boston Univ.	8 months	4 months
Dr. Phil Chamberlin	Collaborator	Univ. Colorado	0	As needed
Dr. Marina Galand	Collaborator	Imperial College, London	0	As needed
Prof. Michael Mendillo	Collaborator	Boston Univ.	0	As needed

Development of a Mars ionosphere model with time-dependent solar forcing for studies of solar flare effects

1 - Introduction

We propose to develop a Mars ionosphere model with time-dependent solar forcing and to use it to compare predictions and observations of the ionospheric effects of solar flares. Solar flares are "active experiments" that probe the response of the martian ionosphere to extreme conditions. The proposed improvements will strengthen one of the weakest areas in current models, the bottomside ionosphere. The Mars ionosphere represents the interface between the neutral atmosphere, driven by seasonal obliquity and dust cycles, and the space plasma environment, driven by the solar wind and crustal magnetic fields. Many escaping particles come from the ionosphere, making ionospheric processes important for the history of volatiles on Mars. Solar flares can impact mission operations because they cause increased radio wave absorption, which impacts communications

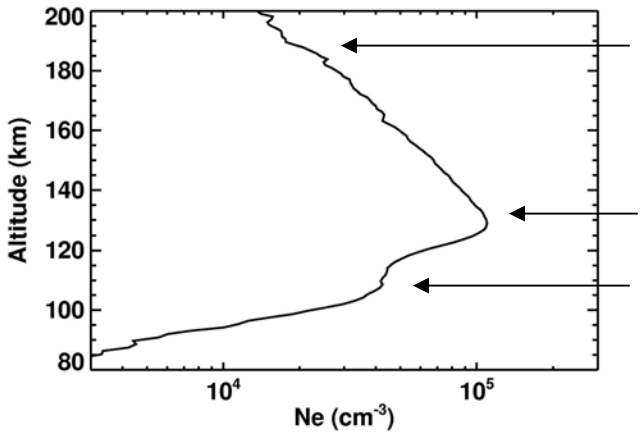

Topside. Mixture of O^+ and O_2^+ ions, controlled by plasma transport

Main layer. O_2^+ ions, controlled by photoionization from 10-100 nm EUV photons.

Lower layer. O_2^+ ions, controlled by photoelectron-impact ionization after photoionization by 1-10 nm X-ray photons.

Fig 1. Sample Ne(z) profile from MGS.

The Mars ionosphere has a lower layer, a main layer, and a topside (Fig 1; Hanson et al., 1977; Chen et al., 1978). The lower layer has also been called the M1 or E layer and the main layer has also been called the M2 or F1 layer (Fox, 2004; Rishbeth and Mendillo, 2004). The main layer is formed where 10-100 nm EUV photons ionize CO_2 molecules to produce CO_2^+ ions. These rapidly charge exchange with O atoms, whose mixing ratio is ~1%, to form O_2^+ ions. The O_2^+ ions dissociatively recombine with an electron to form two neutral O atoms. The main layer is controlled by local photochemical processes, not plasma transport, and has a Chapman-like shape. The lower layer is formed where 1-10 nm X-ray photons are absorbed. As these high-energy photons ionize CO_2 to produce CO_2^+ ions, they eject energetic photoelectrons. These make additional CO_2^+ ions by "photoelectron-impact ionization" as they thermalize by collisions with CO_2 molecules.

Although current ionospheric models accurately reproduce Viking Lander ion composition data around the main ionospheric layer (e.g. Shinagawa and Cravens, 1989; Ma et al., 2004; Fox and Yeager, 2006), they fail to reproduce observations of the variable lower layer and bottomside ionosphere for two reasons (Bougher et al., 2001; Fox, 2004). First, lower layer electron densities (Ne) are highly variable on timescales of

hours due to variability of 1-10 nm solar irradiance (Fig 2). Existing planetary ionosphere models use a constant solar spectrum, such as a reference solar maximum spectrum. Second, photoelectron-impact ionization, which creates ~5-10 ions per photon absorbed in the lower layer, is challenging to model accurately and to validate against observations (Fox, 2004). Only a small fraction of lower layer ions are produced by photoionization.

The photochemical timescale in the ionosphere is proportional to 1/Ne. It is a few minutes at the subsolar main layer and less than an hour for Ne>1500 cm^{-3} (~100-200 km for solar zenith angles smaller than 80^{o}). The effects of transport processes on the dayside are minor below ~180 km.

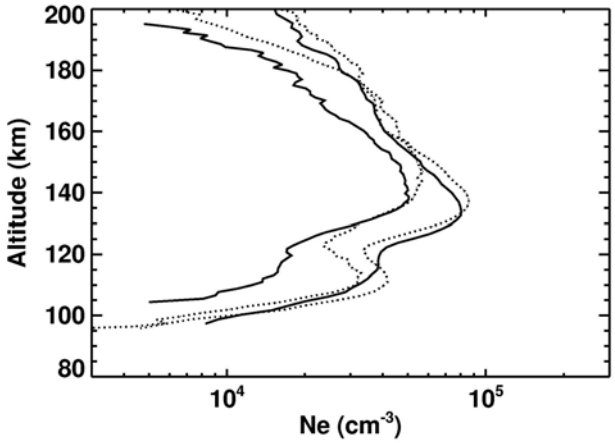

Fig 2. Four MGS profiles showing variability in the shape and size of the lower layer for similar latitude and local solar time.

This proposal describes ionospheric observations during solar flares (Section 2), ionospheric models (Sections 3-5), planned simulations (Sections 6-8), anticipated results (Section 9), and our work plan (Sections 10-13).

Our basic research plan is:
- Adapt existing 1-D Mars ionosphere model to permit time-variable solar irradiances and various models of photoelectron-impact ionization.
- Acquire solar spectra with good spectral and temporal range and resolution.
- Run simulations to produce vertical profiles of ion and electron densities as functions of time.
- Adjust models of photoelectron-impact ionization to optimize fit between observations and simulations.
- Draw conclusions about the effects of solar flares on the Mars ionosphere.
- Draw conclusions about how photoelectron-impact ionization controls the bottomside Mars ionosphere.
- Draw conclusions about the physical process of photoelectron-impact ionization that are transferable to all ionospheres.

2 - Ionospheric Observations During Solar Flares

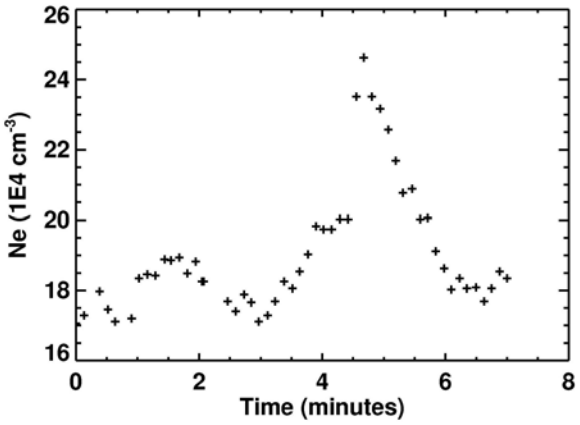

Fig 3. Seven minutes of MARSIS radar sounder data at constant solar zenith angle from 15 Sep 2005. Peak Ne increased from 1.8 x 10^5 cm^{-3} to 2.4 x 10^5 cm^{-3} during an X1.1 solar flare (Gurnett et al., 2005; Nielsen et al., 2006). MARSIS often fails to receive a return signal from the Mars surface (Morgan et al., 2006; Espley et al., 2007). This has been attributed to absorption of radio waves by ionized plasma below the main ionospheric layer. Accurate bottomside ionospheric models are needed to explain why MARSIS observations fail.

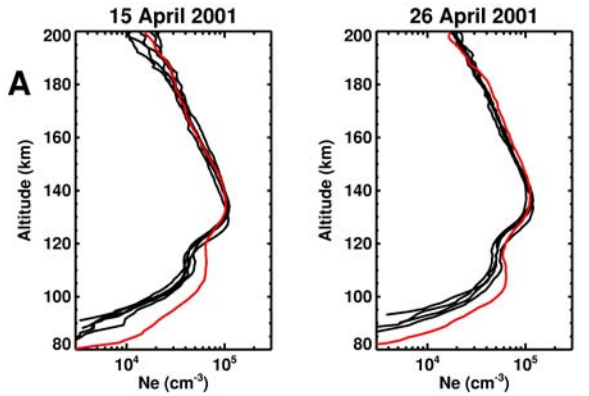

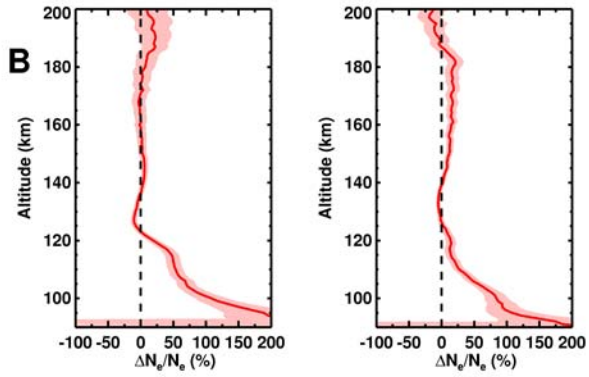

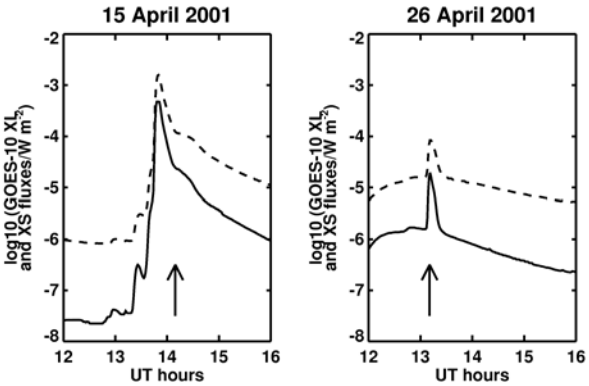

Fig 5. Solar X-ray flux at Earth. GOES XS (solid line, 0.05-0.3 nm) and XL (dashed line, 0.1-0.8 nm) data. Times of MGS Ne(z) are arrowed.

Fig 4. (top) MGS Ne(z) profiles that show increased bottomside Ne during solar flares. (bottom) ΔNe/Ne versus altitude.

The Mars Global Surveyor (MGS) Radio Science (RS) experiment measured 5600 Ne(z) profiles from 1998 to 2006. At least 10 profiles show unusually high Ne in the lower layer at the same time as solar flares were observed from Earth. Two of these cases have been published (Fig 4; Mendillo et al., 2006). Six Ne(z) profiles were observed at two hour intervals on 15 April 2001. Latitude, solar zenith angle, and local solar time were similar for all six profiles. The first five profiles were very similar, but Ne below 120 km were enhanced in the sixth profile. ΔNe/Ne increases as altitude decreases, which is consistent with the hardening of the solar spectrum during flares (Fox and Yeager, 2006).

Solar X-ray observations showed that photons from the peak of an X14.4 flare reached Mars only 20 minutes before the MGS observation was made (Fig 5). The Earth-Sun-Mars angle was only ~26^{o}, so both Earth and Mars were exposed to the flare. A similar event occurred on 26 April 2001, when an MGS observation occurred just as photons from the peak of an M7.8 flare reached Mars.

These new observations make theoretical studies of solar flare effects timely.

Solar flares have a rise timescale ~minutes and a decay timescale ~hours. Ne responds instantly to changes in irradiance. Since the photochemical timescale is short (a few minutes), Ne is effectively controlled by the present irradiance, not the integrated irradiance from the past hour. The neutral atmospheric responds more slowly to the increased heating (increased temperatures, scale heights, and densities). The lack of change in Ne(z) above 120 km in Fig 4 shows that neutral scale heights do not alter in the first 20 mins after a large flare. Therefore models of the ionospheric response to solar flares may use the same neutral atmosphere throughout the simulation. By the time the neutral atmosphere responds to the flare, the ionospheric effects have ceased.

3 - Existing Mars Ionosphere Models

Several 1-D ionospheric models were developed after Viking (Hanson et al., 1977; Chen et al., 1978). Choi et al. (1998) used a 1-D model to show that a downward heat flux is required to explain the Viking Lander ion temperature profile. Ma et al. (2002, 2004) used a 3-D ideal MHD model to study solar wind interaction with Mars. This model included an ionosphere with monochromatic solar irradiance, simplified chemistry, and no photoelectron-impact ionization. Liemohn et al. (2006) used this model to study the behavior of magnetic fieldlines.

Krasnopolsky (2002) developed a 1-D ionospheric model to study the escape of water. Detailed chemistry, high spectral resolution, and photoelectron-impact ionization were included. Several thermospheric general circulation models contain an ionospheric model. Bougher et al. (2001) showed that increasing 1.8-15 nm fluxes by a factor of 10 increased predicted Ne at the lower layer by a factor ~3, consistent with the expected $F \alpha Ne^2$ dependence. A 1-D and 2-D MHD model was developed by Shinagawa and Cravens (1989, 1992). This focused on plasma transport and did not reproduce the lower layer.

Probably the most sophisticated Mars ionosphere model is that of Fox (e.g. Fox and Delgarno, 1979; Fox et al., 1996; Fox, 2004; Fox and Yeager, 2006). This has complex chemistry, high spectral resolution, and detailed photoelectron-impact ionization. It has been used to study the response of the lower layer to solar X-rays (Fox, 2004). This lengthily list may pose the question: Why should NASA support the development of the Boston University Mars Ionosphere Model by funding this proposal?

(1) Only the Fox model and the Boston University Mars Ionosphere Model are currently focused on ionospheric processes and properties. MHD models, e.g. Ma et al. (2004), which are best suited to studies of the ionosphere-magnetosphere interface, have relatively simple ionospheres. The ionospheric model of Krasnopolsky (2002) produced only one paper and that of Bougher et al. (2001) is primarily a support for the neutral thermospheric model.

(2) Parameterizations of photoelectron-impact ionization, once developed in this work, can be implemented in those Mars atmosphere/ionosphere/magnetosphere models that focus on other aspects of the Mars system (e.g. Shinagawa and Cravens, 1992; Bougher et al., 2001; Ma et al., 2004). Since the ionosphere influences the neutral atmosphere and magnetosphere, this would benefit a broad range of Mars research.

(3) The addition of time-varying solar irradiance to this model creates a new and useful capability for planetary ionosphere models.

(4) The model of Fox "cannot reproduce the distinct lower peaks that have been observed in some of the electron density profiles measured by the radio science experiment on the Mars Global Surveyor" despite using a detailed photoelectron collision model (Fox, 2004). Fox (2004), who used a reference Hinteregger solar maximum spectrum,

suggested that adjustments to the X-ray irradiance might fix the problem. Uncertainties in neutral composition or scale height are unlikely to make the simulated lower layer appear as a shoulder, rather than the observed distinct peak. No existing model accurately reproduces observations of the lower layer and bottomside Mars ionosphere.

4 - Boston University Mars Ionosphere Model

Boston University has recently developed a 1-D Mars ionospheric model (Martinis et al., 2003; Mendillo et al., 2003; Withers and Mendillo, 2005; Mendillo and Withers, 2006; Withers et al., 2007). Publications dealing with data analysis have focused on the effects of solar variability on MGS Ne(z) profiles, with timescales that include the 11-year solar cycle, the 28-day solar rotation, day-to-day variability, and hour-long solar flares. Vertical transport of plasma is currently being tested in the model, although this only affects topside Ne, not Ne in the main or lower layers. The main model inputs are neutral atmosphere, solar irradiance, absorption and ionization cross-sections, reaction rates, and a model for photoelectron-impact ionization. We now discuss the current model; proposed changes to the model are discussed in Section 5.

The current 1-D model spans 80-400 km with 1 km vertical resolution. Neutral species include CO_2, O, O_2, N_2, CO, Ar, NO, H_2, H, and He. Number densities of major species for two baseline atmospheres (solar maximum and minimum) come from Bougher's Mars Thermospheric General Circulation Model, as published in Fox et al. (1996). Number densities of minor species were provided by Andrew Nagy (personal communication, 2003). Three aspects of the neutral atmosphere are important: altitude at which the total number density equals some value, such as 10^{11} cm^{-3}, scale height, and composition. Ne(z) is sensitive to the first two. The dominant CO_2->CO_2^+->O_2^+->O+O cycle is not very sensitive to composition. The baseline solar maximum atmosphere has O/CO_2 = 1% at the main layer (130 km) and 0.5% at the lower layer (105 km). Increasing the model's O/CO_2 ratio by a factor of 10 changed subsolar Ne by <2% from 90 to 145 km. Decreasing the model's O/CO_2 ratio by a factor of 10 changed subsolar Ne by <6% from 90 to 160 km. O and CO_2 constitute >90% of the total neutral number density at the main and lower layers, so any changes to minor species abundances have negligible ionospheric effects. The neutral scale height controls the main layer shape and the altitude at which $n=10^{11}$ cm^{-3} controls the main layer altitude (Bougher et al., 2001). If model-data comparisons are poor, these atmospheric properties can be adjusted until the altitude and shape of the main layer are reproduced accurately. From a mathematical perspective, this is equivalent to changing the original altitude scale, z_{old}, to a new one, z_{new}, which satisfies $z_{new} = A + B\ z_{old}$. We do not adjust the composition in any way because uncertainties in the composition have negligible effects on Ne(z).

Solar irradiances are taken from the Solar2000 model (Tobiska et al., 2003; Tobiska, 2004). The spectral range is 1.86 - 105 nm and there are 39 spectral bins (a mixture of regions ~5 nm wide and narrow lines). The shortest wavelength bins, which will be important in this work, are 1.86-2.95 nm, 3.00-4.92 nm, and 5.05-10.00 nm. Solar2000 outputs one solar spectrum at Earth each day. The current ionospheric model does not permit the solar spectrum to vary with time, so a given simulation uses a fixed solar

spectrum, regardless of the simulation's duration. There are no good observations of the solar spectrum at Mars. Observations at Earth do not have spectral ranges and resolutions that are optimized for ionospheric modeling, so even terrestrial models use empirical solar spectra that are derived from observations, such as Solar2000.

Absorption and ionization cross-sections for reactions like CO_2 + hv -> CO_2^+ + e come from a standard source (Schunk and Nagy, 2000). This tabulation matches 37 of Solar2000's 39 wavelength bins. Cross-sections for the 1.86-2.95 nm and 3.00-4.92 nm bins are calculated using analytic expressions (Verner and Yakovlev, 1995; Verner et al., 1996). Cross-sections for molecules are the sum of the cross-sections of the constituent atoms at these wavelengths (Fox et al., 2004). Almost all photons shorter than 20 nm ionize a neutral when they are absorbed, whereas lower-energy photons can be absorbed without ionization.

Ions may undergo chemical reactions before being lost by neutralization. Rate coefficients for reactions like CO_2^+ + O -> O_2^+ + CO and O_2^+ + e -> O + O are taken from a standard source (Schunk and Nagy, 2000). Some rate coefficients depend weakly on electron temperature (Hansen and Mantas, 1988; Choi et al., 1998).

Models of photoelectron-impact ionization are discussed in Section 5.2.

For completeness, we now discuss the underlying structure of the current model. Proposed changes to the model are discussed in the next section.

$$\frac{dN_i}{dt} = \left(P_i^P + P_i^{EI} + P_i^C\right) - \left(L_i^C + L_i^{DR}\right) \quad (1)$$

This is the continuity equation for ion species I^+, as represented by the index i. N_i is the number density of I^+, t is time, P_i^P is the rate of production of I^+ by photoionization, P_i^{EI} is the rate of production of I^+ by photoelectron-impact ionization, P_i^C is the rate of production of I^+ by charge exchange reactions, L_i^C is the rate of loss of I^+ by charge exchange reactions, and L_i^{DR} is the rate of loss of I^+ by dissociative recombination reactions. Four of the five terms on the right-hand side of Eqn 1 are as follows; P_i^{EI} is discussed in Section 5.2. Upper case N refers to ion/electron densities, lower case n to neutral densities.

$$L_i^{DR} = \alpha_i N_i N_e \quad (2)$$

L_i^{DR} is the rate of loss of I^+ in the reaction I^+ + e -> neutral products (e.g. O_2^+ + e -> O + O), and α_i is the relevant rate coefficient. Only molecules can dissociatively recombine.

$$L_i^C = \sum_{s,j,r} k_{isjr} N_i n_s \quad (3)$$

L_i^C is the rate of loss of I^+ in the reaction I^+ + S -> J^+ + R, k_{isjr} is the relevant rate coefficient, and n_s is the number density of neutral species S.

$$P_i^C = \sum_{j,r,s} k_{jris} N_j n_r \quad (4)$$

P_i^C is the rate of production of I^+ in the reaction J^+ + R -> I^+ + S and k_{jris} is the relevant rate coefficient.

$$P_i^P = \sum_{r,\lambda} \sigma_{ion,i,r}(\lambda) n_r(z) F(z,\lambda) \quad (5)$$

P_i^P is the rate of production of I^+ in the reaction R + hv -> I^+ + e, $\sigma_{ion,i,r}$ is the relevant wavelength-dependent ionization cross-section, and F is the flux (photons cm^{-2} s^{-1}) at that altitude (z) and wavelength (λ). F is given by:

$$F(z,\lambda) = F_0(\lambda)\exp(-\tau(z,\lambda)) \quad (6)$$

F_0 is the value of F at the top of the atmosphere and τ is wavelength-dependent optical depth, which is given by:

$$\tau(z,\lambda) = \sum_r \frac{1}{\cos(SZA)} \int_{z'=z}^{z'=\infty} n_r(z') \sigma_{abs,r}(\lambda) dz' \quad (7)$$

SZA is solar zenith angle and $\sigma_{abs,r}$ is the relevant wavelength-dependent absorption cross-section. A more sophisticated calculation of optical depth is used close to the terminator.

There are no spatial derivatives, and therefore no boundary conditions, because plasma transport is not modeled here. Initial conditions are irrelevant because the model is spun-up over several Mars days, which is much longer than the <1 hour dayside photochemical timescale at the main and lower layers.

5 - Proposed Changes to the Model

We wish to better simulate the bottomside Mars ionosphere. This region is critically dependent on how photoelectron-impact ionization is modeled (Section 3), because each photoionization event at these altitudes produces ~5-10 ions via photoelectron impacts (Fox et al., 1996; Fox, 2004). The best way to validate photoelectron-impact ionization models is to compare them to observations, then adjust model parameters until simulations and observations agree. Solar flares are excellent test cases, because observed Ne at altitudes where photoelectron-impact ionization is important are unusually large compared to measurement uncertainties (Mendillo et al., 2006). They also offer the chance to compare simulations and observations both before and during the flare. Thus we study the ionospheric response to solar flares both for its intrinsic scientific value and for its value in illuminating photoelectron-impact ionization. The short timescales associated with solar flares make it necessary to include time-dependent solar irradiances.

We will change the model to include time-varying solar irradiances (Section 5.1) and different models of photoelectron-impact ionization (Section 5.2).

5.1 - Flare Irradiance Spectral Model (FISM) and Cross-Sections

We will use the Flare Irradiance Spectral Model (FISM) (Chamberlin et al., 2004; Chamberlin, 2005; Chamberlin et al., 2005a, 2005b). This model outputs solar irradiance at Earth from 0.5 to 195.5 nm with 1 nm spectral resolution and 1 minute temporal resolution. It is an empirical model that uses reference solar spectra and data from Earth-

orbiting satellites. Data sources include (see Chamberlin, 2005, for descriptions of these datasets):

(A) GOES, 0.05-0.3 nm and 0.1-0.8 nm, 1980s-present,

(B) TIMED SEE, 27-194 nm at 0.4 nm resolution and nine overlapping bands from 0.1-20 nm at ~5 nm resolution, 2002-present,

(C) SOHO SEM, 26-34 nm and 0.1-50 nm, 1995-present,

(D) SNOE SXP, 2-7 nm, 6-19 nm, and 17-20 nm, 1997-2003, and

(E) SOLSTICE instrument on UARS and SORCE, 120-420 nm at 0.5 nm resolution, 1991-present.

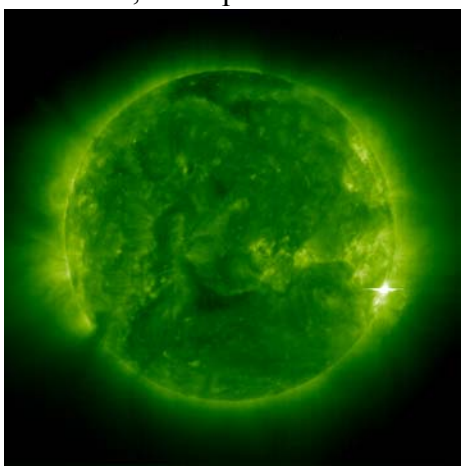

Fig 6. SOHO EIT 19.5 nm image at flare onset on 15 April 2001.

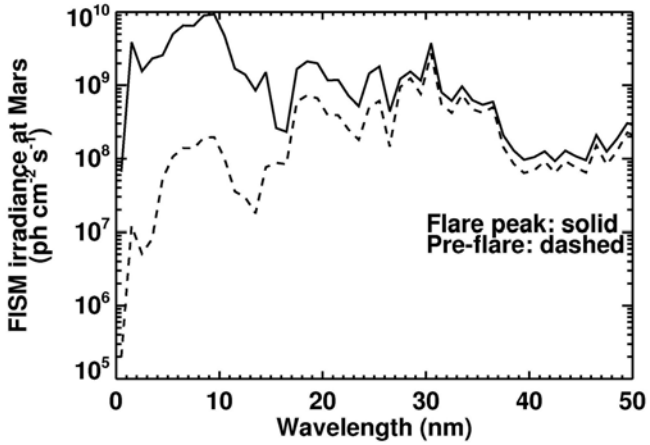

Fig 7. FISM irradiances for 15 April 2001.

The FISM solar spectra will be scaled by $1/R^2$ to account for the different heliocentric distances of Earth and Mars. To minimize the effects of different viewing geometries, we will focus on solar flares that occurred when the Earth-Sun-Mars angle was small and use SOHO EIT 19.5 nm images of the solar disk to ensure that both planets were illuminated by the solar flare (Fig 6 and 7). Spectra will be time-shifted by 4-6 minutes to account for the photon travel time from 1 AU to Mars.

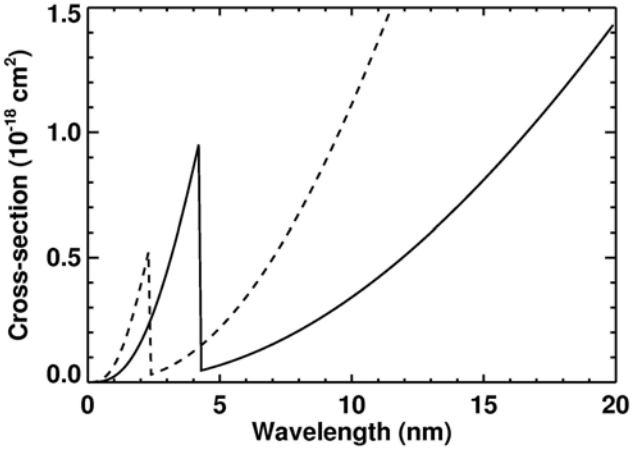

Fig 8. Theoretical ionization cross-sections for C (solid) and O (dashed) (Verner and Yakovlev, 1995; Verner et al., 1996). The cross-section for CO2 is the sum of those for its constituent atoms at these wavelengths ($\sigma_{CO2} = \sigma_C + 2\sigma_o$). Laboratory data for CO_2 with the appropriate spectral range and resolution are not available.

Irradiances and cross-sections must be expressed at the same wavelengths. Absorption and ionization cross-sections in the current model are referenced to 39 wavelength bins (a mixture of regions ~5 nm wide and narrow lines, Section 4). However, cross-sections

vary significantly with wavelength in the 1-10 nm range (Fig 8 and Fox (2004, Fig 12)). These wavelengths control photoionization in the lower layer. The underlying physical reason for the abrupt increase in cross-section with decreasing wavelength is that photons have sufficient energy to eject electrons from the inner electron shells as well as just the outer shell. The three shortest wavelength bins in the current model (1.86-2.95 nm, 3.00-4.92 nm, 5.05-10.00 nm) are too broad to represent these variations accurately.

We use the 0.5 nm, 1.5 nm, ..., 9.5 nm FISM output and generate cross-sections for these wavelengths using the analytical expressions of Verner and Yakovlev (1995) and Verner et al. (1996). These expressions, which rely on molecular cross-sections equaling the sum of the constituent atomic cross-sections, are inaccurate at long wavelenths, so they cannot be used at all FISM wavelengths. We assign the remaining FISM wavelengths to their closest Solar2000 spectral bins and use the usual cross-sections from Schunk and Nagy (2000). Thus we have a composite set of 46 wavelengths for the spectrum and cross-sections. High spectral resolution is used for 10 short wavelengths, where it is needed (Fig 8) and where Verner's cross-section expressions are valid. Standard Solar2000 wavelength bins are used at 36 longer wavelengths to match the available cross-sections. FISM wavelengths >105 nm, longward of the last Solar2000 bin, are neglected because they do not produce ions. FISM results are publicly available at ftp://laspftp.colorado.edu/pub/SEE_Data/fism/. Collaborator Chamberlin will ensure that FISM output for the dates of interest are online, and provide guidance on their use and interpretation.

5.2 - Modeling Photoelectron-Impact Ionization

It is possible to model the energy and trajectory of a photoelectron as it thermalizes by collisions with neutral molecules, tracking how many molecules are ionized in these collisions. Photoelectron collision models have been used in certain terrestrial ionospheric models (e.g. Lummerzheim and Lilensten, 1994; Blelly et al., 1996; and references therein) and in some Venus and Mars ionospheric models (e.g. Kim et al., 1989; Fox, 2004).

However, many terrestrial ionospheric models use a simple scaling factor to represent all photoelectron-impact ionization processes (e.g. Richards and Torr, 1988; Lilensten et al., 1989; Titheridge, 1996). The photoelectron efficiency or primary efficiency, R, is the ratio of the number of ions produced by photoelectron-impact ionization (hard to model) to the number of ions produced by photoionization (easy to model). If R is known, then photoelectron-impact ionization can be modeled as a simple multiplying factor and P_i^{EI} in Eqn 1 can be replaced by R x P_i^{P}. This simplifies the model and, as long as R is chosen correctly, does not impact the model's accuracy.

Two broad statements can be made about R for the wavelengths and altitudes that are relevant here. First, R increases as wavelength decreases, because more energetic photons produce more energetic photoelectrons which require more collisions to thermalize, thereby creating more ion-electron pairs. Second, R increases as altitude decreases, which is due to the greater penetration of high-energy photons. R can be large, with values ~10

being reasonable for 1-10 nm photons. R can in principle depend on the photon energy, the ionization potential and species of the photo-ionized neutral, the composition of the neutral atmosphere, and the ionization potentials of the species in the neutral atmosphere. The vertical distribution of where these photoelectron-impact events produce ions can depend on the scale height and the above properties. Models commonly give R as a function of wavelength and/or altitude and/or species,

The Rees and Jones (1973) parameterization is that an ion-electron pair is created for every 35 eV difference between the energy of the ionizing photon and the neutral species's ionization potential. The ion-electron pair is produced locally, at the same altitude as the photon is absorbed. Since CO_2, not N_2, is the most abundant neutral at Mars ionospheric altitudes, the appropriate value on Mars may be different.

Titheridge (1996) used models of electron collisions to determine R as a function of wavelength and ion species. Values in his Table 3 approximately satisfy R=12 exp(-λ / 7 nm) and do not vary much by species (O^+, O_2^+, N_2^+).

The Richards and Torr (1988) parameterization of R is:

$$R = \frac{A \exp(-\tau)}{\exp(-\tau) + C\sum_i \exp(-D_i \tau)} \qquad (8)$$

where τ is the optical depth at 22.5 nm, $D_i\tau$ approximates the optical depth at λ_i, and A and C are parameters. Richards and Torr (1988) use three λ_i (30, 40, and 50 nm) chosen to represent the full spectrum. Values of D_i are fixed by the ratio of absorption cross-sections at 22.5 nm and λ_i. A and C also have physical significance. At low altitudes, where τ is large, R -> A. At high altitudes, where τ is small, R->A/(1+3C).

Many parameterizations, whether for Venus, Earth, or Mars, have R~0.3 at high altitudes. This value is consistent with detailed photoelectron collision models for the photoionization of neutral molecules (O_2, N_2, CO_2) by 30.4 nm photons, which dominate the ionizing flux at the top of an atmosphere.

These terrestrial parameterizations, since they are all tuned to fit terrestrial observations, lead to similar Ne(z) when implemented in the terrestrial atmosphere. They will lead to dissimilar Ne(z) at Mars, since conditions and composition are different. One major difference between Mars and Earth is the absence of O_2 on Mars. O_2, but not N_2 or CO_2, is ionized by solar Lyman B 102.6 nm photons that do not lead to many photoelectron-impact ionizations. Each photoionization of an O_2 molecule leads to fewer photoelectron-impact ionizations, on average, than for an N_2 or CO_2 molecule, which affects R.

Auger processes can lead to the ejection of two photoelectrons and the formation of a doubly-charged ion when a single soft X-ray photon is absorbed (e.g. Mitchell et al., 2000). Doubly-charged ions form in 10% of cases when soft X-rays ionize O, but only in 1% of cases for CO_2 (Schunk and Nagy, 2000). Auger processes are not included in the current model, but we will perform back-of-the-envelope estimates to consider how they might affect parameterizations of R.

6 - Preliminary Work

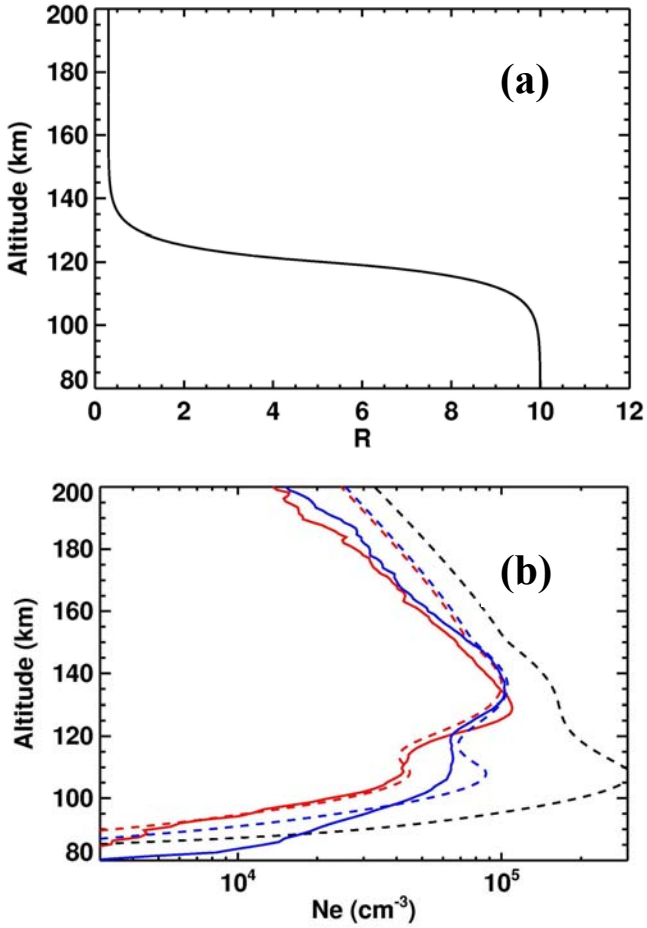

Fig 9. A simple R(z) was used for this demonstration (panel a). It is consistent with Fox et al. (1996).

We have performed three simulations for the 15 April 2001 MGS RS observations using solar irradiances that do not vary with time (panel b). The first case (red) uses irradiances before the flare, the second (black) uses irradiances at the peak of the flare, and the third (blue) uses irradiances from the time of the MGS observation with a large lower layer. Observations are solid lines, simulations are dashed lines. The neutral atmosphere has not been adjusted to reproduce the shape and altitude of the main layer, so the simulated layers are narrower than observed. Ne in the lower layer exceed those in the main layer for the "flare peak" simulation, which is unusual.

The red pre-flare simulation almost matches the shape of the observed lower layer and accurately predicts Ne below 95 km. The blue simulation poorly matches the shape of the lower layer and underpredicts Ne below 95 km. This altitude-dependent model for R shown in Fig 9a works for one case, but not the other. A wavelength-dependent expression for R might be successful in both cases (Section 5.2), because the average wavelength of ionizing photons at a given altitude is shorter during the flare (blue) than before the flare (red). Comparisons like these will be common as we adjust parameterizations of R to improve our simulations, as outlined in Section 7.

7 - Plan of Simulations

Various parameterizations of photoelectron-impact ionization will be tested by comparing simulated and observed Ne(z) profiles. We must first make the changes to the model outlined in Section 5 - incorporating time-varying solar irradiances and different expressions for R. Consistent with terrestrial work, we assume that every ion produced in a cascade of photoelectron-impact ionization is the same species as the ion produced in the initial photoionization event. This assumption is reasonable because photoproduction rates for CO_2^+ far exceed those of other species and CO_2 is the most abundant neutral.

There are at least ten cases when solar flares increased low-altitude Ne in the MGS Ne(z) profiles. We will model each case separately, obtaining model/data comparisons for before and during each flare. The altitude scale in our neutral atmosphere will be adjusted so the main layer altitude and shape are simulated accurately, as discussed in Section 4 (Bougher et al., 2001; Breus et al., 2004). Terrestrial experience and the Mars results of Fox (2004) suggest that R is constant with altitude at and above the main layer, where ionization by 30.4 nm photons is dominant. In this case, main layer shape and altitude are insensitive to whether this constant is 0.1 or 100, so a preliminary simulation with R=constant can be used to adjust the neutral atmosphere. Subsequent optimization of R based on model-data comparisons at lower altitudes will not affect the main layer's shape and altitude. Neutral composition is not adjusted because its effects on simulated Ne(z) are small (Section 4). Since the ionospheric response to a solar flare is over before the neutral atmosphere changes, the same neutral atmosphere will be used throughout each simulation (Section 2).

Task #1: Let the sum of P_i^P over all species be P_{tot}^P and the sum of P_i^{EI} over all species be P_{tot}^{EI}. The total ion production rate at altitude z in the model, $P_{tot,model}$, is $P_{tot}^P + P_{tot}^{EI}$. Let $R_{tot}(z) = P_{tot}^{EI}/P_{tot}^P$ so that $P_{tot,model} = P_{tot}^P \times (1+R_{tot,model})$. The total ion loss rate is proportional to Ne^2 because a single molecular ion species (O_2^+) is dominant at main and lower layer altitudes. On timescales longer than the photochemical timescale, total production and loss rates are equal (Section 1). Therefore $(Ne_{model}/Ne_{obs})^2 = (1+R_{tot,model}) / (1+R_{tot,true})$. Our first set of simulations will use R=0. We will then compare observed and predicted Ne(z), using this equation to estimate $R_{tot,true}(z)$. This estimate will be helpful as we develop general parameterizations in the later Tasks.

Task #2: We assume that all ions produced by photoelectron-impact ionization are produced at the same altitude as the photoionization event. Two different representations for R will be used (Section 5.2): (A) 1 ion-electron pair is produced by photoelectron-impact ionization for every E Joules difference between the photon energy and the ionization potential of the photo-ionized neutral (Rees and Jones, 1973) and (B) $R = X \exp(-\lambda/Y)$ (Titheridge, 1996). Best-fit values of E, X, and Y will be found for each pre-flare and during-flare case. Values of E, X, and Y will be plotted against flare intensity, then against SZA. If the parameters change significantly with flare intensity, then our parameterization is not adequately describing the wavelength dependence of R. If the parameters change significantly with SZA, then our parameterization is not adequately describing how R depends on neutral atmospheric properties that vary with SZA.

Task #3: We anticipate that the best representations found in Tasks #1-2 will be reasonably successful in some cases, but will not be perfect. The third set of simulations will be discovery-driven and will test more complicated parameterizations (Section 5.2). Possible studies include representations like Eqn 8 and distributing the plasma produced by photoelectron-impact ionization over a range of altitudes.

We shall discuss the candidate parameterizations with Collaborator Marina Galand, who is an expert in photoelectron collision models (Galand et al., 1997, 1999, 2006). This will ensure that our candidate parameterizations are physically reasonable and help us relate

values of the fitted parameters to physical properties and processes (Section 5.2). Additional simulations will be performed in Tasks #4-6 to support Tasks #1-3.

Task #4: We wish to gain familiarity with the effects of different parameterizations of photoelectron-impact ionization at the start of this effort (Section 5.2). Simulations with a CO_2-only atmosphere (uniform scale height), simplified chemistry (all CO_2^+ ions instantly converted to O_2^+ ions, loss of O_2^+ ions by dissociative recombination only), and idealized solar irradiances will be performed to study the effects of different parameterizations and different parameter values.

Task #5: We shall simulate the MARSIS observations in Fig 2 and test whether our results for R can reproduce the observed history of Ne,max. We shall determine if Ne,max always corresponded to the main layer or if Ne in the lower layer were greatest for a brief period.

Task #6: Sources of error in the simulations are related to uncertainties in three of the inputs: neutral atmosphere, solar spectrum, and photoelectron-impact parameterization (Sections 4 and 5). In order to estimate the uncertainties in the photoelectron-impact parameters once simulations have been fitted to observations, we must consider the other two sources of error. A series of sensitivity studies will quantify how the best-fit photoelectron-impact parameterization varies with changes such as 25% increase in O/CO_2 ratio, significant changes in the abundances of minor species, or 20% increase in 1-5 nm flux. Uncertainties in observed Ne(z) will also be considered.

8 - Computational Requirements

Each simulation takes ~1 hour to run. Task #1 contains 10 simulations, since there is no optimization of any parameters for the 10 cases. Task #2 contains 800 simulations, calculated assuming 10 cases, 2 different functional forms for photoelectron-impact parameterization, 20 simulations to find the best-fit parameters based on observations, and 2 observed Ne(z) profiles, one pre-flare and one during-flare. Task #3 is likely to contain a similar number. Task #5 requires <10 simulations. Each of Tasks #4 and 6 is likely to require ~100 simulations. The total is <2000 simulations. There is no need for detailed human inspection of the results after every single simulation, so the task is manageable. The only output that must be stored after each simulation is Ne(z) at the appropriate time, which will not pose a storage problem.

9 - Anticipated Results and Broader Implications

We expect that this effort will lead to a validated parameterization of photoelectron-impact ionization on Mars. We will relate the best-fit values of the parameters to physical processes (Section 5.2). Our results for R will be compared to those of other workers. Several Mars ionosphere models that include detailed photoelectron collision models have published figures of the rate of production of ions by (A) photoionization and (B) photoelectron impact as functions of altitude and ion species (Fox et al., 1996; Fox, 2004; Haider et al., 2006). They will also be compared to predictions of R on Venus from the

models of Cravens, Fox, and Nagy (Fox, 2007, and references therein). Since the neutral atmospheres and ionospheric processes are so similar, R may be very similar on Venus and Mars. Results for R in CO_2-dominated atmospheres will then be compared to results for R in N_2-dominated atmospheres (Earth and Titan) to see how sensitive R is to atmospheric composition (Galand et al., 1999; Lilensten et al., 2005). The influence of O_2 in the terrestrial atmosphere may be important (Fig 7 of Titheridge et al., 1996).

Our results for R will consist of simple equations with several parameters. These can easily be used by other workers in their ionospheric models, so dissemination of our results to the broader community is straight-forward. Once any differences between our observationally-validated results for R and those of Fox (2004) are understood, it will be possible to determine why the detailed photoelectron collision model in Fox (2004) failed to reproduce the structure of the lower layer and bottomside ionosphere (Section 3). Thus a successful photoelectron-impact parameterization will help improve detailed photoelectron collision models and their required inputs.

Plasma in the terrestrial ionosphere is accelerated upwards at all altitudes by a solar flare because of changes in the plasma pressure gradient (Mendillo and Evans, 1974). Once photoelectron-impact ionization is adequately modeled by this effort, studies of the effects of solar flares on plasma transport and escape in the Mars ionosphere will be a natural next step for us.

10 - Relevance to NASA Programs

This effort addresses NASA Strategic Sub-goals 3B and 3C (Table 1 of the ROSES NRA). This effort is relevant to MEPAG Goal II (Understanding the processes and history of climate on Mars), Objective A (Characterize Mars's atmosphere), Investigation 1 (Determine the present state of the neutral/ionized upper atmosphere). This effort is directly related to the scientific objectives of the 2011 Mars Scout orbiter - escape processes and the upper atmospheric reservoir available for escape.

11 - Personnel

Principal Investigator Paul Withers will serve as leader of this effort. He has worked extensively on the Mars neutral atmosphere and ionosphere. Recent projects include a study of the relationship between variability in the Sun's EUV flux due to its 27 day rotation and Mars Ne(z), analysis of Mars ionospheric observations during a solar flare, and the use and development of this Mars ionospheric model. His funded effort will be 4 months per year. An MDAP grant to Boston University (PI Mendillo), awarded in 2007, will support his ongoing analysis of ionospheric observations of solar flare effects, which will be beneficial to this effort.

This proposal includes an application by PI Withers for an Early Career Fellowship. Withers received his PhD in 2003. In addition to a strong publication record, Withers has served on NASA/NSF review panels, reviewed PDS datasets, been a Huygens Science Team member, and been a member of Spirit's Atmospheric Advisory Group for Landing.

Graduate Student Majd Matta will play a substantial role in this project. She entered Boston University's Astronomy PhD program in fall 2007 and is currently using ionospheric models, including this Mars model, to compare the ionospheres of Venus, Earth, and Mars. As a non-Caucasian female scientist, her participation will help NASA's efforts to increase diversity amongst scientists active in planetary exploration. Funds are budgeted to ensure that Graduate Student Matta, not just PI Withers, attends scientific conferences. Matta's effort will be 12 months per year. We request funds for 8 months per year here. Funds for the remaining 4 summer months will be provided by Boston University's Center for Space Physics.

Collaborator Phil Chamberlain (University of Colorado) will ensure that FISM results are available for dates of interest. He will also advise on the general topic of 1-10 nm solar irradiance. Collaborator Marina Galand (Imperial College, London) will ensure that we use reasonable functions for photoelectron-impact parameterization. She will also advise on the physical significance of the parameters. Collaborator Michael Mendillo (Boston University) will be Graduate Student Matta's academic advisor, which will ensure an active role for him. He will also advise on comparative aeronomy, including the terrestrial ionosphere and its response to solar flares (Mendillo and Evans, 1974; Mendillo et al., 1974). As stated in their letters of commitment, the collaborators' levels of effort will be sufficient to fulfill their responsibilities. Collaborators will be invited to Boston for several days each year with travel funds supplied by the University's Center for Space Physics.

12 - Cost effectiveness

We believe that this is a cost-effective proposal. Most of the funded work-hours will be provided by a graduate student, with the rest provided by a post-doctoral researcher. 4 months of the graduate student's effort will be provided at no cost to this grant. Three collaborators, experts in topics of importance for this work, will provide guidance and data products at no cost to this grant. Preliminary work developing the model has already been performed and many flare-affected Ne(z) profiles have already been identified.

13 - Work Plan

Matta's effort will be focused on changing the model (Section 5), running simulations (Section 7) and interpreting the results. Withers's effort will be focused on defining the inputs for each simulation and interpreting the results.
Year 1: Tasks #1, #4, and implement time-varying irradiances in model.
Year 2: Tasks #2, #5.
Year 3: Tasks #3, #6, and comparisons and analysis discussed in Section 9.

References

Blelly, P.-L., Lilensten, J., Robineau, A., Fontanari, J., and Alcayde, D. (1996) Calibration of a numerical ionospheric model with EISCAT observations, Ann. Geophys., 14, 1375-1390.

Bougher, S., Engel, S., Hinson, D., and Forbes, J. (2001) Mars Global Surveyor radio science electron density profiles: Neutral atmosphere implications, Geophys. Res. Lett, 28, 3091-3094.

Bougher, S. W., Roble, R. G., and Fuller-Rowell, T. (2002) Simulations of the upper atmospheres of the terrestrial planets, in *Atmospheres in the Solar System: Comparative Aeronomy*, Geophys. Monogr. Ser., 130, eds. M. Mendillo, A. Nagy, J. H. Waite, AGU, Washington, DC.

Bougher, S. W., Engel, S., Hinson, D. P., and Murphy, J. R. (2004) MGS Radio Science electron density profiles: Interannual variability and implications for the martian neutral atmosphere, J. Geophys. Res., 109, E03010, doi:10.1029/2003JE002154.

Bougher, S. W., Bell., J. M., Murphy, J. R., Lopez-Valverde, M. A., and Withers, P. (2006) Polar warming in the Mars thermosphere: Seasonal variations owing to changing insolation and dust distributions, Geophys. Res. Lett., 33, L02203, doi:10.1029/2005GL024059.

Breus, T. K., Krymskii, A. M., Crider, D. H., Ness, N. F., Hinson, D., and Barashyan, K. K. (2004) Effect of the solar radiation in the topside atmosphere/ionosphere of Mars: Mars Global Surveyor observations, J. Geophys. Res., 109, A09310, doi:10.1029/2004JA010431.

Chamberlin, P. C., Woods, T. N., and Eparvier, F. G. (2004) Flare Irradiance Spectral Model (FISM) A model of solar vacuum ultraviolet irradiance over timescales from flares to solar cycles, Fall AGU meeting, abstract #SM13B-02.

Chamberlin, P. C. (2005) The Flare Irradiance Spectral Model (FISM). PhD dissertation, University of Colorado, available online at ftp://laspftp.colorado.edu/pub/SEE_Data/fism

Chamberlin, P. C., Woods, T. N., and Eparvier, F. G. (2005a) First results from the Flare Irradiance Spectral Model (FISM): A model of solar vacuum ultraviolet irradiance over timescales from flares to solar cycles, Spring AGU meeting, abstract #SA23A-12.

Chamberlin, P. C., Woods, T. N., and Eparvier, F. G. (2005b) Comparisons of new Flare Irradiance Spectral Model (FISM) to current solar ultraviolet irradiance measurements, Fall AGU meeting, abstract #SA34A-08.

Chen, R. H., Cravens, T. E., and Nagy, A. F. (1978) The martian ionosphere in light of the Viking observations, J. Geophys. Res., 83, 3871-3876.

Choi, Y. W., Kim, J., Min, K. W., Nagy, A. F., and Oyama, K. I. (1998) Effect of the magnetic field on the energetics of Mars ionosphere, Geophys. Res. Lett., 25, 2753-2756.

Espley, J. R., Farrell, W. M., Brain, D. A., Morgan, D. D., Cantor, B., Plaut, J. J., Acuña, M. H., Picardi, G. (2007) Absorption of MARSIS radar signals: Solar energetic particles and the daytime ionosphere, Geophys. Res. Lett., 34, L09101, doi:10.1029/2006GL028829.

Fox, J. L., and Delgarno, A. (1979) Ionization, luminosity, and heating of the upper atmosphere of Mars, J. Geophys. Res., 84, 7315-7333.

Fox, J. L, Zhou, P., and Bougher, S. W. (1996) The Martian Thermosphere/Ionosphere at High and Low Solar Activities, Adv. Space Res., 17(11) 203-218.

Fox, J. L. (2004) Response of the martian thermosphere/ionosphere to enhanced fluxes of solar X-rays, J. Geophys. Res., 109, A11310, doi:10.1029/2004JA010380.

Fox, J. L., and Yeager, K. E. (2006) Morphology of the near-terminator martian ionosphere: A comparison of models and data, J. Geophys. Res., 111, A10309, doi:10.1029/2006JA011697.

Fox, J. L. (2007) Near-terminator Venus ionosphere: How Chapman-esque?, J. Geophys. Res., 112, E04S02, doi:10.1029/2006JE002736.

Galand, M., Lilensten, J., Kofman, W., Sidje, R. B. (1997) Proton transport model in the ionosphere 1. Multistream approach of the transport equations, J. Geophys. Res., 102, 22261-22272.

Galand, M., Lilensten, J., Toublanc, D., and Maurice, S. (1999) The ionosphere of Titan: Ideal diurnal and nocturnal cases, Icarus, 140, 92-105.

Galand, M., Yelle, R. V., Coates, A. J., Backes, H., and Wahlund, J.-E. (2006) Electron temperature of Titan's sunlit ionosphere, Geophys. Res. Lett., 33, L21101, doi:10.1029/2006GL027488.

GOES (2006) http://goes.ngdc.noaa.gov/data/

Gurnett, D. A., Kirchner, D. L., Huff, R. L., Morgan, D. D., Persoon, A. M., Averkamp, T. F., Duru, F., Nielsen, E., Safaeinili, A., Plaut, J. J., Picardi, G. (2005) Radar soundings of the ionosphere of Mars. Science, 310, 1929-1933.

Haider, S. A., Seth, S. P., Choksi, V. R., and Oyama, K. I. (2006) Model of photoelectron impact ionization within the high latitude ionosphere at Mars: Comparison of calculated and measured electron density, Icarus, 185, 102-112.

Hanson, W. B., Sanatani, S., and Zuccaro, D. R. (1977) The martian ionosphere as observed by the Viking Retarding Potential Analyzer, J. Geophys. Res., 82, 4351-4363.

Hanson, W. B., and Mantas, G. P. (1988) Viking electron temperature measurements - evidence for a magnetic field in the martian ionosphere, J. Geophys. Res., 93, 7538-7544.

Kim, J., Nagy, A. F., Cravens, T. E., and Kliore, A. J. (1989) Solar cycle variations of the electron densities near the ionospheric peak of Venus, J. Geophys. Res., 94, 11997-12002.

Krasnopolsky, V. A. (2002) Mars' upper atmosphere and ionosphere at low, medium, and high solar activities: Implications for evolution of water, J. Geophys. Res., 107, E12, 5128, doi:10.1029/2001JE001809.

Krymskii, A. M., Ness, N. F., Crider, D. H., Breus, T. K., Acuna, M. H., and Hinson, D. P. (2004) Solar wind interaction with the ionosphere/atmosphere and crustal magnetic fields at Mars: Mars Global Surveyor Magnetometer/Electron Reflectometer, radio science, and accelerometer data, J. Geophys. Res., 109, A11306, doi:10.1029/2004JA010420.

Liemohn, M. W., Ma., Y., Frahm, R. A., Xiaohua, F., Kozyra, J. U., Nagy, A. F., Winningham, J. D., Sharber, J. R., Barabash, S., Lundin, R. (2006) Mars global MHD predictions of magnetic connectivity between the dayside ionosphere and the magnetospheric flanks, Space Sci. Rev., 126, 63-76.

Lilensten, J., Kofman, W., Wisemberg, J., Oran, E. S., and Devore, C. R. (1989) Ionization efficiency due to primary and secondary photoelectrons: A numerical model, Ann. Geophys., 7, 83-90.

Lilensten, J., Simon, C., Witasse, O., Dutuit, O., Thissen, R., and Alcaraz, C. (2005) A fast computation of the diurnal secondary ion production in the ionosphere of Titan, Icarus, 174, 285-288.

Lummerzheim, D., and Lilensten, J. (1994) Electron transport and energy degradation in the ionosphere: Evaluation of the numerical solution, comparison with laboratory experiments and auroral observations, Ann. Geophys., 12, 1039-1051.

Ma, Y, Nagy, A. F., Hansen, K. C., DeZeeuw, D. L., and Gombosi, T. I. (2002) Three-dimensional multispecies MHD studies of the solar wind interaction with Mars in the presence of crustal fields, J. Geophys. Res., 107, doi:10.1029/2002JA009293.

Ma, Y., Nagy, A. F., Sokolov, I. V., and Hansen, K. C. (2004) Three-dimensional, multispecies, high spatial resolution MHD studies of the solar wind interaction with Mars, J. Geophys. Res., 109, A07211, doi:10.1029/2003JA010367.

Martinis, C. R., Wilson, J. K., and Mendillo, M. (2003) Modeling day-to-day ionospheric variability on Mars, J. Geophys. Res., 108, A10, 1383, doi:10.1029/2003JA009973.

Mendillo, M., and Evans, J. V. (1974) Incoherent scatter observations of the ionospheric response to a large solar flare, Radio Sci., 9, 197-203.

Mendillo, M., and 14 colleagues (1974) Behavior of the ionospheric F-region during the great solar flare of August 7, 1972, J. Geophys. Res., 79, 665-672.

Mendillo, M., Smith, S. M., Wilson, J. K., Rishbeth, H., and Hinson, D. P. (2003) Simultaneous ionospheric variability on Earth and Mars, J. Geophys. Res., 108, doi:10.1029/2003JA009961.

Mendillo, M., Pi, X., Smith, S. M., Martinis, C., Wilson, J., and Hinson, D. (2004) Ionospheric effects upon a satellite navigation system at Mars, Radio Sci., 39, RS2028, doi:10.1029/2003RS002933.

Mendillo, M., Withers, P., Hinson, D., Rishbeth, H., and Reinisch, B. (2006) Effects of solar flares on the ionosphere of Mars, Science, 311, 1135-1138.

Mendillo, M., and Withers, P. (2006) Effects of solar flares on Earth and Mars, Spring AGU meeting, abstract U52A-02.

Mitchell, D. L., Lin, R. P., Rème, H., Crider, D. H., Cloutier, P. A., Connerney, J. E. P., Acuña, M. H., and Ness, N. F. (2000) Oxygen Auger electrons observed in Mars' ionosphere, Geophys. Res. Lett., 27, 1871-1874.

Morgan, D. D., Gurnett, D. A., Kirchner, D. L., Huff, R. L., Brain, D. A., Boynton, W. V., Acuña, M. H., Plaut, J. J., and Picardi, G. (2006) Solar control of radar wave absorption by the martian ionosphere, Geophys. Res. Lett., 33, L13202, doi:10.1029/2006GL026637

Neupert, W. M. (2006) Variability of the solar soft X-ray irradiance (0.6-2.5 nm) with solar activity, Adv. Space Res., 37, 238-245.

Nielsen, E., Zou, H., Gurnett, D. A., Kirchner, D. L., Morgan, D. D., Huff, R., Orosei, R., Safaeinili, Plaut, J. J., and Picardi, G. (2006) Observations of vertical reflections from the topside martian ionosphere, Space Sci. Rev., 126, 373-388.

Rees, M. H., and Jones, A. V. (1973) Time dependent studies of the aurora 2. Spectroscopic morphology, Planet. Space Sci., 21, 1213-1235.

Richards, P. G., and Torr, D. G. (1988) Ratios of photoelectron to EUV ionization rates for aeronomic studies, J. Geophys. Res., 93, 4060-4066.

Rishbeth, H., and Mendillo, M. (2004) Ionospheric layers of Mars and Earth, Planet. Space. Sci., 52, 849-852, 2004.

Schunk, R., and Nagy, A., (2000) *Ionospheres: Physics, Plasma Physics, and Chemistry*, Camb. Univ. Press., NY.

Shinagawa, H., and Cravens, T. E. (1989) A one-dimensional multispecies magnetohydrodynamic model of the dayside ionosphere of Mars, J. Geophys. Res., 94, 6506-6516.

Shinagawa, H., and Cravens, T. E. (1992) The ionospheric effects of a weak intrinsic magnetic field at Mars, J. Geophys. Res., 97, 1027-1035.

Simon, C., Witasse, O., Leblanc, F., Lilensten, J., Mouginot, J., Kofman, W., and Bertaux, J.-L. (2007) Analysis and modelling of SPICAM data onboard Mars Express, EGU meeting, EGU2007A-06650.

Sutton, E. K., Forbes, J. M., Nerem, R. S., and T. N. Woods (2006) Neutral density response to the solar flares of October and November, 2003, Geophys. Res. Lett., 33, L22101, doi:10.1029/2006GL027737.

Titheridge, J. E. (1996) Direct allowance for the effect of photoelectrons in ionospheric modeling, J. Geophys. Res., 101, 357-369.

Tobiska, W. K., Woods, T., Eparvier, F., Viereck, R., Floyd, L., Bouwer, D., Rottman, G., and White, O. R. (2000) The SOLAR2000 empirical solar irradiance model and forecast tool, J. Atmos. And Solar-Terr. Phys., 62, 1233-1250.

Tobiska, W. K. (2004) SOLAR2000 irradiances for climate change research, aeronomy, space systems engineering, Adv. Space Res., 34, 1736-1746.

Verner, D. A., and Yakovlev, D. G. (1995) Analytic fits for partial photoionization cross sections, Astronomy and Astrophysics Supplement Series, 109, 125-133.

Verner, D. A., Ferland, G. J., Korista, K. T., and Yakovlev, D. G. (1996) Atomic data for astrophysics II. New analytic fits for photoionization cross sections of atoms and ions, Astrophys. J., 465, 487-498.

Witasse, O., Blelly, P.-L., Lilensten, J., Leblanc, F. (2006) TRANSMARS, a kinetic-fluid model of the martian ionosphere, European Planetary Science Congress, EPSC2006-A-00011.

Withers, P., Bougher, S. W., and Keating, G. M. (2003) The effects of topographically-controlled thermal tides on the martian upper atmosphere as seen by the MGS accelerometer, Icarus, 164, 14-32.

Withers, P., Mendillo, M., Rishbeth, H., Hinson, D. P., and Arkani-Hamed, J. (2005) Ionospheric characteristics above martian crustal magnetic anomalies, Geophys. Res. Lett., 32, L16204, doi:10.1029/2005GL023483.

Withers, P., and Mendillo, M. (2005) Response of peak electron densities in the martian ionosphere to day-to-day changes in solar flux due to solar rotation, Planet. and Space Sci., 53, 1401-1418.

Withers, P. (2006) Mars Global Surveyor and Mars Odyssey accelerometer observations of the martian upper atmosphere during aerobraking, Geophys. Res. Lett., 33, L02201, doi:10.1029/2005GL024447.

Withers, P., Wroten, J., Mendillo, M., Chamberlin, P., and Woods, T. (2007) Modeling the effects of solar flares on the ionosphere of Mars, European Geophysical Union Annual Meeting, abstract EG2007-A-05089.

Biographical Sketch for PI Paul Withers

Center for Space Physics
Boston University
725 Commonwealth Avenue
Boston MA 02215

Tel: (617) 353 1531
Fax: (617) 353 6463
Email: withers@bu.edu
Citizenship: British

Education

- PhD, Planetary Science, University of Arizona 2003
- MS, Physics, Cambridge University, Great Britain 1998
- BA, Physics, Cambridge University, Great Britain 1998

Recent Professional Experience

- Research associate Dr. Michael Mendillo (Boston Univ) 2003-present
  Analysis of ionospheric data from Mars and Earth, plus numerical modelling
- Graduate research assistant Dr. Stephen Bougher (Univ. of Arizona) 1998 – 2003
  Studied weather in the martian upper atmosphere. Played an advisory role in mission operations for Mars Global Surveyor and Mars Odyssey aerobraking

Fellowships, Honors, and Awards

- CEDAR Postdoctoral Fellowship from NSF for upper atmospheric research 2003
- Kuiper Memorial Award from the University of Arizona for excellence in academic work and research in planetary science. 2002

Selected Peer Reviewed Publications and Other Major Publications

- Crosby, Bothmer, Facius, Griessmeier, Moussas, Panasyuk, Romanova, and **Withers** "Interplanetary Space Weather and its Planetary Connection" (2007) *Space Weather*, under review.
- Christou, Vaubaillon, and **Withers** "The dust trail complex of comet 79P/du Toit-Hartley and meteor outbursts at Mars" (2007) *Astronomy and Astrophysics*, in press.
- **Withers** "A technique to determine the mean molecular mass of a planetary atmosphere using pressure and temperature measurements made by an entry probe: Demonstration using Huygens data" (2007) *Planetary and Space Science*, 55, in press, 10.1016/j.pss.2007.04.009.
- Montabone, Lewis, Read, and **Withers** "Reconstructing the weather on Mars at the time of the MERs and Beagle 2 landings" (2006) *Geophysical Research Letters*, 33, L19202, doi:10.1029/2006GL026565.
- **Withers** and Smith "Atmospheric entry profiles from the Mars Exploration Rovers Spirit and Opportunity" (2006) Icarus, 185, 133-142, doi:10.1016/j.icarus.2006.06.013.
- Mendillo, **Withers,** Hinson, Rishbeth, and Reinisch "Effects of solar flares on the ionosphere of Mars" (2006) *Science*, 311, 1135-1138.

- Bougher and 4 colleagues, including **Withers** "Polar warming in in the Mars thermosphere: Seasonal variations owing to changing insolation and dust distributions" (2006) *Geophysical Research Letters*, 33, L02203, doi:10.1029/2005GL024059.

- **Withers** "Mars Global Surveyor and Mars Odyssey Accelerometer observations of the martian upper atmosphere during aerobraking" (2006) *Geophysical Research Letters*, 33, L02201, doi:10.1029/2005GL024447.

- Fulchignoni and 42 colleagues, including **Withers** "In situ measurements of the physical characteristics of Titan's environment" (2005), *Nature*, **438**, 785-791, doi:10.1038/nature04314.

- **Withers** and Mendillo "Response of peak electron densities in the martian ionosphere to day-to-day changes in solar flux due to solar rotation" (2005) *Planetary and Space Science*, **53**, 1401-1418, doi:10.1016/j.pss.2005.07.010.

- **Withers** "What is a planet?" (2005) *Eos*, **86**(36), 326, doi:10.1029/2005EO360004.

- **Withers**, Mendillo, Rishbeth, Hinson, and Arkani-Hamed "Ionospheric characteristics above Martian crustal magnetic anomalies" (2005) *Geophysical Research Letters*, **32**, L16204, doi:10.1029/2005GL023483.

- **Withers**, Bougher, and Keating, "The Effects of Topographically-Controlled Thermal Tides in the Martian Upper Atmosphere as seen by the MGS Accelerometer", (2003) *Icarus*, **164,** 14-32.

- **Withers**, Towner, Hathi, and Zarnecki, "Analysis of entry accelerometer data: A case study of Mars Pathfinder", (2003) *Planetary and Space Science*, **51,** 541-561.

- **Withers** and Neumann, "Enigmatic northern plains of Mars" (2001) *Nature*, **410**, 651.

- **Withers**, "Meteor storm evidence against the recent formation of lunar crater Giordano Bruno" (2001) *Meteoritics and Planetary Science*, **36**, 525 – 529.

Professional Activities and Service

• Reviewer of MER, MRO, Huygens, and Rosetta for NASA PDS and ESA	2004 - present
• Review panel member for NASA Mars Data Analysis Program, NASA Planetary Atmospheres Program, NASA Venus Express Participating Scientist Program, NASA Mars Fundamental Research program, NSF Astronomy and Astrophysics Research Grants Program	2004 - present
• Reviewer for Advances in Space Research, Annales Geophysicae, Icarus, Journal of Geophysical Research, Journal of Spacecraft and Rockets, Mars, Meteoritics and Planetary Science, Planetary and Space Science, and Science.	2001 - present
• Funded co-investigator on NASA Mars Scout Phase A grant for "The Great Escape" mission	2007
• Huygens SSP and HASI/ACC Team Member	2005 - present
• NASA 2003 Mars Exploration Rovers – Atmospheric Advisory Team.	2002 – 2004
• Beagle 2 Environmental Sensor Suite Team Member	2001 - 2003

Professional Affiliations: Member of the American Geophysical Union's Planetary Sciences Section, the American Astronomical Society's Division for Planetary Science, and the British Planetary Forum.